JOURNAL OF SPACECRAFT AND ROCKETS
Vol. 44, No. 1, January–February 2007

Identification of Tethered Satellites with Mixed Observational Data

Steven G. Tragesser*
University of Colorado, Colorado Springs, Colorado 80933
and
Mark Faulstich†
Air Force Space Command, Schriever AFB, Colorado 80912-7383

DOI: 10.2514/1.22291

Tethered satellite systems present a challenge to tracking systems and software, because the end bodies do not follow Keplerian motion. For very long tethers, the motion of the end body can be more consistent with a suborbital vehicle than an orbiting satellite. Therefore, a robust and efficient algorithm is warranted that can identify if a satellite is tethered. This research develops an approach that estimates the tether length by minimizing an objective function of the residual errors between measured and estimated position. Tethered satellite identification is then based on the estimated tether length. A unique feature of the filter is that it permits mixed observations of either end mass, but there is no a priori knowledge of which body is associated with any given data point. This "data sorting" problem is a necessary component of any practical system. The methodology presented here is tested with data from the Tether Physics and Survivability Experiment.

Nomenclature

a, e, i, ω, Ω	=	orbital elements of the tether system center of mass
J_2	=	harmonic coefficient for Earth's oblateness
L	=	tether length
M	=	mean anomaly of the tether system center of mass
m	=	mass
$\hat{\boldsymbol{P}}, \hat{\boldsymbol{Q}}, \hat{\boldsymbol{W}}$	=	perifocal coordinate frame basis along periapsis, semilatus rectum, and orbit normal
p	=	semilatus rectum of the tether system center of mass
$\boldsymbol{R}$	=	position vector of the tracking site
R	=	radius of the Earth
$\boldsymbol{r}$	=	position vector from the center of the Earth to the satellite
$\hat{\boldsymbol{S}}, \hat{\boldsymbol{E}}, \hat{\boldsymbol{Z}}$	=	topocentric coordinate frame basis along the local south, east, and vertical
$T_{\mathrm{SEZ}/PQW}$	=	transformation matrix from the topocentric coordinate frame to the perifocal frame
α	=	azimuth angle from tracking site to satellite
ε	=	elevation angle from tracking site to satellite
ν	=	true anomaly
$\boldsymbol{\rho}$	=	postion vector from the tracking site to the satellite
σ_r	=	variance of the radial distance to the satellite
σ_ε	=	tracking site variance of elevation
σ_ρ	=	tracking site variance of slant range

Subscripts

est	=	based on mathematical model
obs	=	based on observational data
o	=	value of parameter at initial time
t	=	tether
1	=	lower body of tether system
2	=	upper body of tether system

I. Introduction

EXTENSIVE research has been accomplished in recent years to determine a quick, reliable method for identifying whether an object in space is part of a tethered satellite system (TSS) [1–8]. The motivation for this activity stems largely from the problem that under certain conditions, end bodies could appear to a conventional tracking system as though they are on a suborbital trajectory [1]. The main challenges of tethered object identification are the non-Keplerian motion of the tether end bodies and that the radar returns can come from either of the end bodies. Most of the focus has been on the first issue. For example, [2,3] estimate the tether force on a tracked object. If the estimated force is above a certain threshold, then it is assumed that the object is part of a TSS because a single-body satellite should not have this force present. A multistage approach to tether identification and orbit prediction has also been developed [4] as well as a genetic algorithm estimator [5].

The previous research generally assumes, however, that the data points fed into the filter all come from the same object or that the end body associated with a given data point is known. A more capable system, however, must allow for radar returns from either end body and for the "tagging" of this data (association of a measurement with a particular end mass) to be uncertain. This "data sorting" issue became apparent with the data analysis of the Tether Physics and Survivability experiment (TiPS) [9]. Using the large amount of data (including satellite laser ranging and optical images), the team was able to very accurately determine the orbit and behavior of the tether and two end bodies. It was estimated that approximately 30% of the data was mistagged. Obviously, any identification algorithm would need a way to identify mistagged data in order to obtain an accurate and reliable solution. Although previous approaches may partially account for this problem by throwing out large residuals, the approach presented here provides a way to sort the data within the filter so that mistagged data may be retained to optimize filter performance.

The measurement data used for this research consist of range, azimuth and elevation, as would be obtained from a radar tracking station.

Received 5 January 2006; accepted for publication 13 August 2006.

*Assistant Professor, Department of Mechanical and Aerospace Engineering, 1420 Austin Bluffs Parkway. Senior Member AIAA.

†Flight Commander, Force Enhancement Flight, 17th Test Squadron, 730 Irwin Avenue, Suite 83.

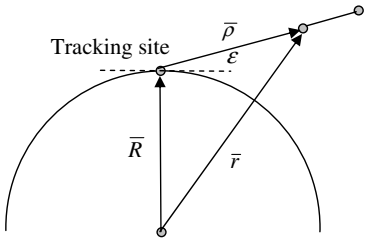

Fig. 1 Observation geometry of one of the end bodies.

II. Data Sorting

The parameter used to unambiguously tag each measurement to one of the end bodies is the radial distance from the center of the Earth. If the orbit is perfectly known and the measurements are accurate, this parameter provides an unambiguous criterion for determining which of the two bodies was observed as long as the tether libration is less than 90 deg. A radial distance less than the orbit radial distance (assumed to be coincident with the tether center of mass) would indicate an observation of the lower end body. Conversely, a radial distance greater than the orbit would indicate an observation of the upper mass. This paradigm is the basis for the data sorting algorithm. Referring to Fig. 1, the radial distance to the observed object is calculated based on one tracking observation using the expression

$$r = \sqrt{\rho^2 - R^2 + 2\rho R\cos(90^\circ + \varepsilon)} \tag{1}$$

Both the slant range and elevation are typically available from a radar tracking site.

A disadvantage using the radial distance is that its value is very sensitive to observation errors at low elevations. Assuming the errors in range and elevation are uncorrelated, the uncertainty in the radial distance is

$$\sigma_r^2 = J\begin{bmatrix} \sigma_\rho^2 & 0 \\ 0 & \sigma_\varepsilon^2 \end{bmatrix} J^T \tag{2}$$

where

$$J = \begin{bmatrix} \frac{\partial r}{\partial \rho} & \frac{\partial r}{\partial \varepsilon} \end{bmatrix} \tag{3}$$

The elements $\frac{\partial r}{\partial \rho}$ and $\frac{\partial r}{\partial \varepsilon}$ are obtained by taking the partial derivatives of Eq. (1) with respect to ρ and ε, respectively. These partials are

$$\frac{\partial r}{\partial \rho} = \frac{\rho - R\cos(90^\circ + \varepsilon)}{\sqrt{R^2 + \rho^2 - 2R\rho\cos(90^\circ + \varepsilon)}} \tag{4}$$

$$\frac{\partial r}{\partial \varepsilon} = \frac{-R\rho\sin(90^\circ + \varepsilon)}{\sqrt{R^2 + \rho^2 - 2R\rho\cos(90^\circ + \varepsilon)}} \tag{5}$$

To illustrate how these uncertainties can cause errors in the data sorting algorithm, consider an example of a 2 km nadir-oriented tether satellite in a 7400 km orbit which is observed by a tracking station with a performance given by $\sigma_\rho = 0.02$ km and $\sigma_\varepsilon = 0.025$ deg. For equal mass end bodies, the radial distances to the lower mass are 7399 km and 7401 km to the upper mass as shown in Fig. 2. The uncertainty for different observation geometries (i.e., elevation angles) as calculated from Eq. (2) is also plotted. The uncertainty envelope becomes quite large for the lower elevation observations. In fact, this $1-\sigma$ uncertainty envelope overlaps at an elevation of 9 deg. This implies a 16% likelihood that an observation of the lower mass will have a calculated radial distance *greater* than the center of mass and will therefore be incorrectly sorted by this algorithm. This accuracy in the data sort assumes that the orbit is perfectly known. Errors in the orbit will further degrade the data sort performance.

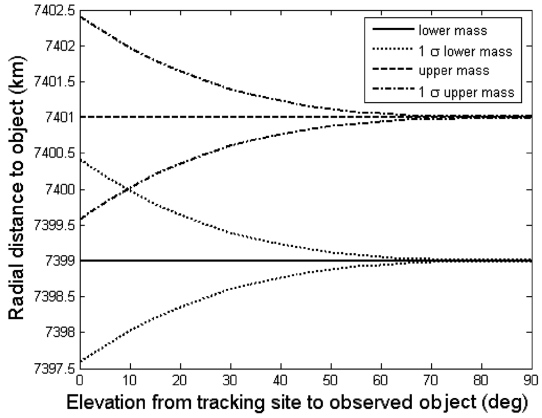

Fig. 2 1σ errors in the radial distance for a given radar site performance.

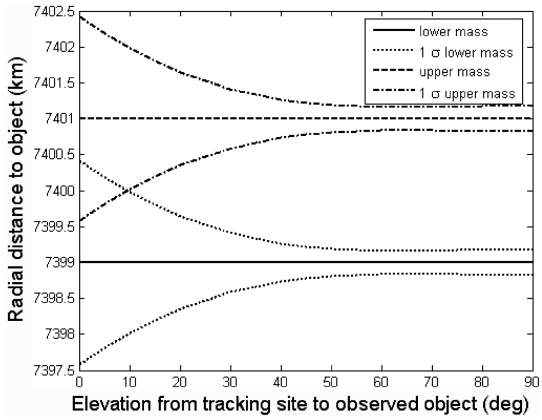

Fig. 3 1σ errors in the radial distance for reduced range performance.

For reasonable values of the radar performance, the expected accuracy of the data sort is driven by the uncertainty in the elevation angle measurement. To illustrate, the uncertainty in radial distance is plotted in Fig. 3 for $\sigma_\rho = 0.2$ km and $\sigma_\varepsilon = 0.025$ deg. This order of magnitude increase in range uncertainty mainly affects the larger elevation measurements. It does not substantially alter the point at which the uncertainty envelope intersects the cm distance and, therefore, does not change the accuracy of the data sort for this level of angle precision.

Tether oscillation causes additional problems when distinguishing between the radial distance to the end bodies. For this reason, the performance of this method will be somewhat reduced for large amplitude tether oscillations.

III. Identification/Estimation Approach

The tether identification algorithm is based on estimating the orbit of the TSS center of mass and the tether length using radar tracking data. The estimation method used for this research can be decomposed into three main tasks. The first step involves taking the observed azimuth, elevation, and slant range data from a tracking site and determining an initial estimated set of orbital elements. The second main piece of the estimator is the calculation of the residuals, that is, the difference between the estimate and the measurement. To calculate the residuals, the estimated orbit elements of the tethered system are propagated forward and the position vectors of the end bodies are expressed in the perifocal coordinate frame. A simple rigid tether following perturbed Keplerian motion is used to model the end body motion (see Fig. 1). The estimated end body positions are then differenced with the calculated position from the observation data to determine the residuals. This calculation requires that the observation be associated with a particular end body via the data sorting algorithm discussed above. The third main piece of the

estimator is MATLAB optimization software to iterate on the orbit elements and the tether length to minimize the residuals. Each of these pieces is described in more detail below.

A. Initial Estimate

The initial estimate of the system center of mass orbit is accomplished with a Herrick–Gibbs algorithm [10]. This algorithm is for a point mass object, and so using the measurements from the end bodies (displaced from the center of mass) does not yield a very accurate solution. However, this initial estimate proved to be an adequate initial guess for the optimization scheme discussed below. This technique uses three Earth-centered position vectors to determine the orbit. To calculate these vectors, the position vector from the tracking station to the observed object is first obtained in the topocentric-horizon coordinate system (SEZ) from the range, elevation, and azimuth measurements:

$$\boldsymbol{\rho}_{\text{obs}} = \rho\cos\varepsilon\cos\alpha\hat{\boldsymbol{S}} + \rho\cos\varepsilon\sin\alpha\hat{\boldsymbol{E}} + \rho\sin\varepsilon\hat{\boldsymbol{Z}} \tag{6}$$

This vector is converted to the Earth-centered inertial (ECI) frame and added to the ECI position of the tracking site to get the observed position vector of the object as shown in Fig. 1:

$$\boldsymbol{r}_{\text{obs}} = \boldsymbol{R} + \boldsymbol{\rho}_{\text{obs}} \tag{7}$$

To get the results to match observational data, the flattening of the Earth must be included in the calculation of the tracking site position.

The Herrick–Gibbs algorithm yields an estimate of the velocity for the second observation time. The estimated velocity and the observed position are then used to calculate the estimated osculating orbit elements.

B. Residual Calculation

The system dynamics is modeled as a rigid tether aligned with the local vertical following perturbed Keplerian motion. Obviously this will not be the state of an actual system, but tether librations should be small for most missions. For TiPS, the libration amplitude was between 30–40 deg after deployment. After less than a year, this amplitude decayed down to approximately 5–7 deg [11]. The system center of mass is assumed to coincide with the center of gravity; that is, the center of mass motion is assumed identical to a particle of the same mass. The center of mass motion is assumed to follow two-body motion with the only perturbation considered to be that of the Earth's oblateness. Neglecting the effect that the distributed mass has on the orbital motion will introduce additional error in the filter for very long tethers. Drag may need to be considered for some applications, but TiPS is at a sufficiently high altitude that this perturbation was not significant.

Given these assumptions, the center of mass motion is given by the following set of time-varying orbit elements [12]:

$$\begin{aligned} &a(t) = a_o \qquad i(t) = i_o \qquad e(t) = e_o \\ &\omega(t) = \omega_o + \frac{3}{2}\frac{J_2}{p^2}\bar{n}(t-t_o)\left(2 - \frac{5}{2}\sin^2 i\right) \\ &\Omega(t) = \Omega_o - \frac{3}{2}\frac{J_2}{p^2}\bar{n}(t-t_o)\cos i \qquad M(t) = M_o + \bar{n}(t-t_o) \end{aligned} \tag{8}$$

where $\bar{n}$ is the perturbed mean motion given by the following:

$$\bar{n} = \sqrt{\frac{\mu}{a^3}}\left[1 + \frac{3}{2}\frac{J_2\sqrt{1-e^2}}{p^2}\left(1 - \frac{3}{2}\sin^2 i\right)\right] \tag{9}$$

From the orbit elements, the center of mass position in the perifocal coordinate system is

$$\boldsymbol{r}_{\text{est}} = \frac{a(1-e^2)}{1+e\cos\nu}(\cos\nu\hat{\boldsymbol{P}} + \sin\nu\hat{\boldsymbol{Q}}) \tag{10}$$

where the true anomaly is calculated by solving Kepler's equation (see, for example, [13]). A tolerance of 1×10^{-15} is used to determine convergence of Kepler's equation. The optimization scheme described below performed better with the residuals expressed in this frame. The estimated positions of the end masses are easily calculated for the assumption of a vertical tether:

$$\boldsymbol{r}_{1\,\text{est}} = \boldsymbol{r}_{\text{est}} - \frac{m_t L + 2m_2 L}{2(m_1+m_2+m_t)}(\cos\nu\hat{\boldsymbol{P}} + \sin\nu\hat{\boldsymbol{Q}}) \tag{11}$$

$$\boldsymbol{r}_{2\,\text{est}} = \boldsymbol{r}_{\text{est}} + \frac{m_t L + 2m_1 L}{2(m_1+m_2+m_t)}(\cos\nu\hat{\boldsymbol{P}} + \sin\nu\hat{\boldsymbol{Q}}) \tag{12}$$

The position vector at a given observation time based on the measurements is given by Eq. (7). This vector is then converted to the perifocal coordinate frame:

$$\boldsymbol{r}_{\text{obs}} = [T_{\text{SEZ}/PQW}](\boldsymbol{R} + \boldsymbol{\rho}_{\text{obs}}) \tag{13}$$

where $T_{\text{SEZ}/PQW}$ is obtained from the tracking site location and the estimated orbital elements in Eq. (8).

To calculate the residual between the observation and estimate, the data sorting algorithm is employed. The difference in the magnitude of the observation and estimate for both of the end masses was compared. The observation is tagged to whichever end body was closer to the estimate. Therefore the position residuals are expressed as

$$\text{Residual} = \sqrt{\sum_{i=1}^{n} |(\bar{r}_{\text{obs}})_i - (\bar{r}_{k\text{est}})_i|^2} \tag{14}$$

where $(\,)_i$ denotes the ith observation and

$$k = \begin{cases} 1 & \text{if } \|\bar{r}_{\text{obs}}| - |\bar{r}_{1\,\text{est}}\| < \|\bar{r}_{\text{obs}}| - |\bar{r}_{1\,\text{est}}\| \\ 2 & \text{if } \|\bar{r}_{\text{obs}}| - |\bar{r}_{1\,\text{est}}\| > \|\bar{r}_{\text{obs}}| - |\bar{r}_{2\,\text{est}}\| \end{cases} \tag{15}$$

C. Optimization

The center of mass orbit and the tether system parameters are estimated by minimizing the residuals. The states are the initial orbit elements, the tether length, and the ratio of the end body masses. The tether mass is assumed to be negligible for the estimation algorithm. Therefore, the end body positions in Eqs. (11) and (12) can be expressed solely in terms of the mass ratio m_1/m_2. Thus, the eight states a_o, e_o, i_o, ω_o, Ω_o, M_o, L, and m_1/m_2 completely characterize the behavior of the end masses under the given assumptions. The objective function will append a term to the residual in Eq. (14) to penalize errors in the radial distance to the observed body. This is already implicitly included in Eq. (15); however, trial-and-error demonstrated that a significant weighting on these errors increased the robustness and convergence speed of the optimization. A factor of 10 weighting was found to yield good performance. The final objective function is

$$\begin{aligned} &\Phi(a_o, e_o, i_o, \omega_o, \Omega_o, M_o, L, m_1/m_2) \\ &\quad = \sqrt{\sum_{i=1}^{n} |(\bar{r}_{\text{obs}})_i - (\bar{r}_{k\text{est}})_i|^2 + 10\|(\bar{r}_{\text{obs}})_i| - |(\bar{r}_{k\text{est}})_i\|^2} \end{aligned} \tag{16}$$

This function is minimized using "fmincon" in version seven of the MATLAB optimization toolbox. This algorithm uses a gradient-type search direction along with a one-dimensional line search to minimize the objective function subject to any constraints. There are no constraints active for this problem. The algorithm is determined to have converged when the change in the norm of the directional derivative of the function is below a specified tolerance. The default tolerance of 1×10^{-6} was used for the results presented below. Other optimization algorithms could also be applied to this problem to enhance the performance of the filter.

IV. Results

The algorithm was validated with data from three different sources: an in-house simulator, the commercial tether simulation package TetherSim™, and observations of the TiPS experiment.

A. In-House Simulator

1. Baseline Case

The in-house simulator uses the same model as the estimation and identification algorithm, namely, a rigid tether aligned along the local vertical with center of mass motion governed solely by two-body motion with J_2 perturbations. The errors in the observations are assumed to be Gaussian with zero mean. The variances assumed for the range, elevation, and azimuth are $\sigma_\rho = 0.05$ km, $\sigma_\varepsilon = 0.02°$, and $\sigma_\rho = 0.02°$. The tether system is based upon the parameters for TiPS. The tether length is 4.023 km, the lower mass is 43.3 kg, the upper mass is 10.2 kg, and the tether mass is 5.5 kg. The initial orbit elements of the center of mass are

$$a_o = 7400 \text{ km} \quad e_o = 0.004 \quad i_o = 65.3° \quad \omega_o = 70.0° \quad \Omega_o = 220.45° \quad \nu_o = 70.0° \tag{17}$$

A data arc of 200 s is used to test the algorithm, with observations every 10 s. At each observation, the simulator randomly selects between the lower and upper end bodies for the measurement data. The radial distances computed for uncorrupted and noisy observations are shown on Fig. 4 using the symbols "*" and "×," respectively.

The initial orbit determination is accomplished with the Herrick–Gibbs algorithm using the first three observations. As shown in Fig. 4, these data are composed of one lower mass observation and two upper mass observations. As a result, the initial estimate is not very accurate:

$$(a_o)_{\text{est}} = 7453 \text{ km} \quad (e_o)_{\text{est}} = 0.010 \quad (i_o)_{\text{est}} = 65.41° \quad (\omega_o)_{\text{est}} = 107.74° \quad (\Omega_o)_{\text{est}} = 220.36° \quad (\nu_o)_{\text{est}} = 32.86° \tag{18}$$

Using this estimate as an initial guess in the MATLAB optimization routine, the objective function in Eq. (16) is minimized. After a computation time of 6 s, the final center of mass orbit estimate is

$$(a_o)_{\text{est}} = 7399.6 \text{ km} \quad (e_o)_{\text{est}} = 0.0044 \quad (i_o)_{\text{est}} = 65.29° \quad (\omega_o)_{\text{est}} = 67.98° \quad (\Omega_o)_{\text{est}} = 220.46° \quad (\nu_o)_{\text{est}} = 72.02° \tag{19}$$

These estimates are all fairly close to the true values except for the argument of perigee and true anomaly. However, the sum of these two values for both the estimate and the true orbit is equal to 140 deg. This effect is due to the inherent difficulty in resolving the argument of perigee for a nearly circular orbit.

The tether length estimate was 3.79 km. This represents an error of approximately 6% and correctly indicates that this is a tethered system. The estimated radial distances of the end masses are shown in Fig. 4 with the symbols ▽ and ◇. There is generally good agreement between the end mass position and the observations. All of the 21 observations are correctly sorted to the appropriate end body. Note that if the observations are not corrupted with noise, the orbit and tether estimates almost perfectly match the truth (e.g., the tether length estimate is 4.02 km) as can be observed from the correlation between the perfect observations and the estimates with perfect data in Fig. 4.

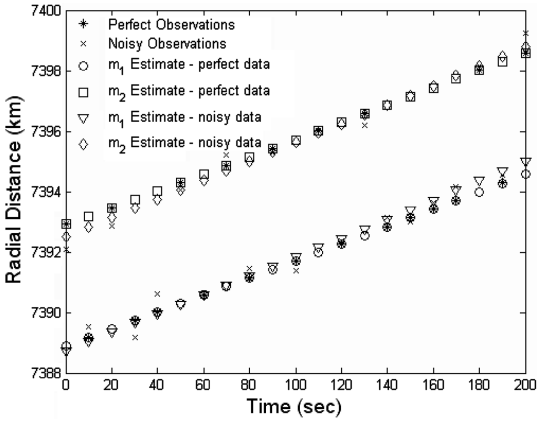

Fig. 4 Comparison of observations and final estimate for in-house simulation.

A Monte Carlo analysis was performed for the baseline parameters, as well as for increased measurement noise. Orbit and tether estimates were calculated for 100 simulations with randomly generated measurements. The mean and variance for the estimated semimajor axis and tether length are given in Table 1 for the baseline and increased error levels of 2, 3, and 4 times the baseline values. The performance of the filter is seen to generally degrade as the error levels increase. However, in all of these cases, the satellite is correctly identified as tethered.

The percentage of objects that the filter attributes to the incorrect end body is also listed in Table 1. These numbers are much larger than predicted by the error analysis based on Eq. (2), because that prediction assumes a perfectly known orbit. To illustrate, the 2σ uncertainty in radial distance is given in Fig. 5 for the error levels that are 3 times the baseline. The elevation of the observations in the Monte Carlo simulation are all at or above the 29 deg threshold for distinguishing between the upper and lower masses as obtained from the plot. Therefore, the error analysis predicts that less than 2.3% of the observations should be incorrectly sorted using radial distance. The mean percentage of incorrectly sorted observation of 5.4% is much larger than this theoretical value. Improved filter algorithms could potentially increase the actual filter performance closer to the theoretical maximum.

2. Single-Body Satellite

To demonstrate that the estimation algorithm can correctly identify untethered vehicles, observations for a single satellite were generated with the in-house simulator. The initial orbital and tracking site errors are the same as the baseline case. The estimation process gave back very good estimates of the orbit elements for the center of mass for this case, and, more important, it identified that the center of mass was approximately zero kilometers away from the observed object. This near zero distance implies that the body is a single, untethered satellite.

One potential weakness of the identification algorithm is evident if a tether system has a large portion of the mass all in one end body

Table 1 Monte Carlo results for baseline and increased error levels

	Semimajor axis mean/variance, km	Tether length mean/variance, km	Mean % of incorrectly sorted observations	% of objects identified as tethered
Truth	7400	4.02	——	——
Baseline	7398.3/1.5	4.01/0.18	0	100
2× error levels	7399.6/2.3	4.02/0.33	0.1	100
3× error levels	7401.4/4.2	4.12/0.45	5.4	100
4× error levels	7403.9/5.3	4.39/0.53	11.2	100

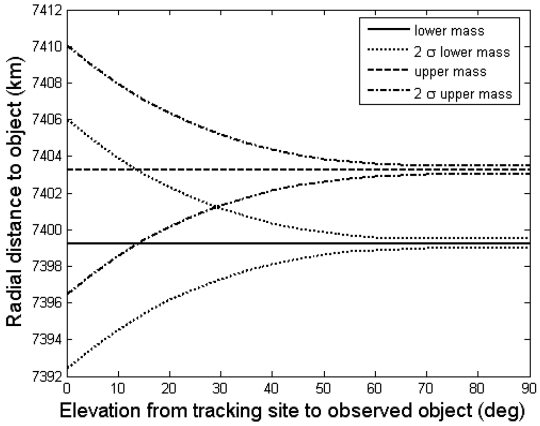

Fig. 5 Uncertainty in observations for 3 times the error of the baseline case.

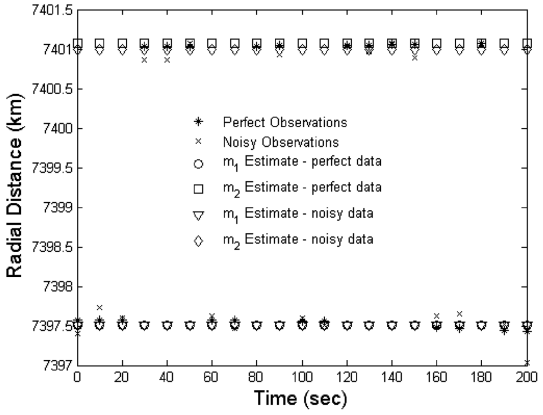

Fig. 6 Comparison of observations and final estimate for TetherSim™ data.

such that the center of mass is very near that mass. Typically, the more massive body would also have a much larger radar cross section, and so the smaller mass would not be observed. The system will not appear to be tethered because the trajectory of the observed end mass is nearly Keplerian.

B. TetherSim™ Data

TetherSim™ uses a much higher fidelity model than the in-house simulator [14]. The gravity model includes spherical harmonics up through 8th order as well as lunar perturbations. Tether libration and flexibility effects are modeled with the "implicit" propagator which uses a finite element method.

The same orbit as the examples above was used in the TetherSim™ simulations. However, the timing (and therefore the pass geometry) differs such that the elevation angles were more favorable. A Monte Carlo simulation was performed with randomly generated measurement noise added to TetherSim™ simulations with varying libration angles. The main impact of the libration on the estimate, as seen in Table 2, is upon the tether length. The libration of the tether is simply offset by a shorter estimate of the tether. In fact, the tether estimates found in the third column are seen to be nearly proportional to the cosine of the libration angle. An example of this phenomenon is shown in Fig. 6 for the 30 deg libration case. Unlike the in-house simulation results, the modeling errors in the TetherSim™ examples cause the estimate and observations to differ even for perfect measurements as shown in Fig. 6.

As would be expected, there is significant degradation in the filter performance at very large libration angles where the radial distance is reduced to levels that are difficult to distinguish due to the measurement errors. This leads to the large number of satellites that are not identified as tethered in the 60 deg libration case.

C. Tether Physics and Survivability Data

Tracking data for TiPS from July 1997 are analyzed. This specific set of tracking data was selected because of the favorable tracking site viewing geometry. Even with the favorable geometry for this tracking site pass, the highest elevation angles obtained from the site were approximately 67 deg, while the lowest elevation angle was approximately 3 deg.

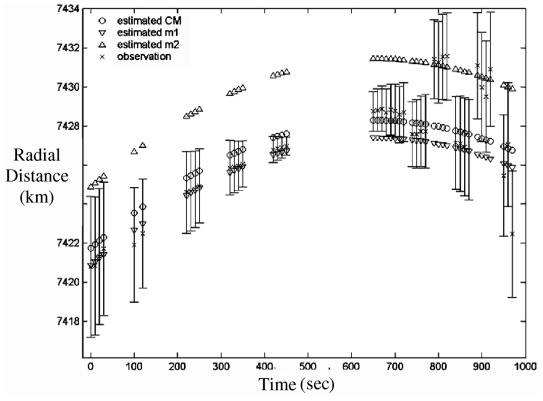

Fig. 7 Comparison of observations and final estimate for TiPS data

The parameters of the TiPS system are given above in the baseline case. One unique characteristic of the system is a dipole antenna sewn into the tether. This dipole is less than 100 m away from the center of mass (CM), which adds to the challenge of correctly identifying the source object of an observation.

Figure 7 shows the comparison of the observations with the estimated positions of the end bodies and the center of mass. Error bars are plotted to indicate 3σ uncertainty for each of the data points. These uncertainties are estimated using Eq. (2). The estimation algorithm also seems to have performed well with the actual TiPS data. Here we do not have a truth model to measure the performance of the filter, but the close correspondence between the estimated data and the observational data is encouraging. For example, the observational data are right on top of the estimated position of the lower mass between 200 and 500 s, when the tracking geometry was favorable.

The figure seems to indicate all of the observations taken before 500 s are observations of the lower mass. After the large time gap in the middle is when it appears the tracking site started to observe the center of mass and the upper mass. The results of this figure show how important data sorting is when dealing with a TSS because it is obvious that not all of the observations are of the same end mass, even though all of the data were supposed to be from the lower end mass.

Table 2 Monte Carlo results for varying libration amplitudes

	Semimajor axis mean/variance, km	Tether length mean/variance, km	Mean % of incorrectly sorted observations	% of objects identified as tethered
Truth	7400	4.02	——	——
0° libration	7396.8/1.7	3.99/0.06	0	94
7° libration	736.5/2.3	3.97/0.06	0	97
30° libration	7397.3/2.2	3.55/0.07	0	96
60° libration	7397.2/6.1	2.24/0.12	0.4	60

V. Conclusion

Experience gained from the Tether Physics and Survivability experiment shows that tether the identification or the orbit determination algorithm must take into account improperly tagged observation data. The simple approach for autonomously sorting tracking data that was developed in this work seems to accurately deal with this problem except when the tracking geometry is very poor (below about 10 deg elevation, depending on the radar site performance).

References

[1] Lovell, T. A., Cho, S., Cochran, J. E., and Cicci, D. A., "Use of Tethered Satellite Estimation Methods in Identifying Re-Entering Objects," *Advances in the Astronautical Sciences*, Vol. 105, No. 2, 2000, pp. 1427–1442.

[2] Choe, N. J., Jo, J. H., and Cochran, J. E., "Detection of Tethered Satellite Systems," *Journal of the Astronautical Sciences*, Vol. 52, Nos. 1–2, Jan./June 2004, pp. 93–106.

[3] Cicci, D. A., Lovell, T. A., and Qualls, C., "A Filtering Method for the Identification of a Tethered Satellite," *Journal of the Astronautical Sciences*, Vol. 49, No. 2, April–June 2001, pp. 309–326.

[4] Cicci, D. A., Cochran, J. E., Qualls, C., and Lovell, T. A., "Quick-Look Identification and Orbit Determination of a Tethered Satellite," *Journal of the Astronautical Sciences*, Vol. 50, No. 3, July–Sept. 2003, pp. 339–353.

[5] Lovell, T. A., "Application of Genetic Algorithms to State Estimation of Tethered Systems," *Computer Methods in Applied Mechanics and Engineering*, Vol. 192, No. 15, April 2003, pp. 1799–1819.

[6] Cochran, J. E., Cho, S., Lovell, T. A., and Cicci, D. A., "Evaluation of the Information Contained in the Motion of One Satellite of a Two-Satellite Tethered System," *Journal of the Astronautical Sciences*, Vol. 48, No. 4, Oct.–Dec. 2000, pp. 477–493.

[7] Cochran, J. E., Cho, S., Lovell, T. A., and Cicci, D. A., "Modeling Tethered Satellite Systems for Detection and Orbit Determination," *Journal of the Astronautical Sciences*, Vol. 49, No. 1, Jan.–March 2001, pp. 89–108.

[8] Alfriend, K. T., Barnds, W. J., Coffey, S. L., and Stuhrenberg, L. M., "Attitude and Orbit Determination of a Tethered Satellite System," *Advances in the Astronautical Sciences*, Vol. 90, No. 1, 1996, pp. 831–848.

[9] Barnds, W. J., and Coffey, S. L., "Tracking of the TiPS Tethered Satellite System," *Advances in the Astronautical Sciences*, Vol. 103, No. 2, 1999, pp. 1843–1853.

[10] Bate, R. R., Mueller, D. D., and White, J. E., *Fundamentals of Astrodynamics*, Dover Publications, Inc., New York, 1971, pp. 109–116.

[11] Barnds, W., Coffey, S., Davis, M., Kelm, B., and Purdy, W., "TiPS: Results of a Tethered Satellite Experiment," *Advances in the Astronautical Sciences*, Vol. 97, Astrodynamics Part I, Univelt, Inc., San Diego, CA, 1997, pp. 3–23.

[12] Vallado, D. A., *Fundamentals of Astrodynamics and Applications*, McGraw–Hill, New York, 1997, pp. 579–586.

[13] Wiesel, W. E., "Spaceflight Dynamics," 2nd ed., Irwin/McGraw–Hill, New York, 1997, pp. 579–586

[14] Hoyt, R. P., "TetherSim™ User Manual," Tethers Unlimited, Inc., Lynnwood, WA, Sept. 2003.

D. Spencer
Associate Editor